State-Specific Vibrational Relaxation and Thermal Dissociation in Nonequilibrium Hypersonic Flows

Eswar Josyula* and William F. Bailey†

*Air Force Research Laboratory, Wright-Patterson Air Force Base, Ohio 45433, U.S.A.
†Air Force Institute of Technology, Wright-Patterson Air Force Base, Ohio 45433, U.S.A.

Abstract. Numerical simulations are presented of steady state, hypersonic blunt body nitrogen flow for conditions under which there is considerable thermal dissociation. The objective is to understand the thermodynamic nonequilibrium phenomena encountered along the trajectory of hypersonic aerospace vehicles. The internal energy relaxation processes of vibrational energy transfer, dissociation and recombination were treated using state-to-state kinetics of diatomic nitrogen. The state-specific rates were incorporated into a solution of the master kinetic equations coupled to the fluid dynamic equations to describe the thermo-chemical nonequilibrium phenomenon in high temperature hypersonic flowfields. The influence of multi-quantum vibrational energy exchange was assessed for vibrational heating and cooling conditions. The nonequilibrium vibrational energy distributions were evaluated under multiple-quantum vibrational-translational (VT) and vibration-vibration (VV) energy exchanges. The competing effects of resonant and non-resonant VV exchanges and VT de-excitation rates were studied for flow conditions with Treanor distributions, typically encountered in expanding nozzles. For simulations of vibrational cooling flows with double quantum transitions, additional up-pumping of energy in the intermediate quantum levels was observed due to enhanced VV exchanges. Results of the dissociating flowfield simulations were compared with two dissociation models for nitrogen, (a) Park model and (b) depletion model. The state-specific dissociation and recombination rates were employed in the study of vibrational bias and depletion effects. Vibrational bias was strong for both the dissociation and recombination processes in nitrogen at temperatures ranging from 6,000 to 20,000 K. The shock-standoff distance of the full state-kinetic implementation and the depletion model were consistent with each other and resulted in a greater shock-standoff distance compared with the Park model for a Mach 19 nitrogen flow past a hemisphere cylinder of radius 0.1524 m.

INTRODUCTION

The presence of shock waves in high speed flow of air presents considerable difficulties for accurate numerical simulation of the flowfield. The shock wave redistributes the high kinetic energy of the oncoming flow into various internal energy modes, which relax relatively slowly, leading to significant chemical and thermal nonequilibrium in the stagnation region. In the gas kinetic description, intermolecular collisions change the translational, rotational, vibrational, and electronic energies of the collision partners. The probabilities of these elementary processes differ significantly, giving rise to widely separate relaxation times for the internal modes. Thus it becomes important to account for the rates of relaxation processes to predict the nonequilibrium behavior of these kinds of flows.

For nonequilibrium hypersonic flow calculations in the continuum flight regime, the translational and rotational mode are assumed to be in thermodynamic equilibrium and are designated with a single tanslational-rotational temperature. However, the vibrational relaxation process with its slower relaxation time scales stays in a state of nonequilibrium in the high altitude hypersonic flowfields. Hypersonic codes routinely use Landau-Teller model to describe the vibrational relaxation and assign a single vibrational temperature to characterize the vibrational temperature. However, at higher vibrational energies when there is thermal dissociation of the diatomic molecules, there are serious modeling difficulties to simulate the dissociation process from a single vibrational temperature based on the Landau-Teller relaxation model. Generally, the rate-controlling temperature to determine the Arrhenius rates for dissociation is taken to be the geometric mean of the translational-rotational temperature and the single vibrational temperature. This model known as the Park model [1] is used in hypersonic codes today due to its simplicity. However, the Park model lacks a physical basis and has been shown to be inaccurate for a wide range of temperatures [2].

In recent years several studies were attempted to model the vibrational kinetics and dissociation using state-to state kinetic models. See for example Refs. [3, 4]. In the state-kinetic modeling, the processes of vibration-translation (V-T),

vibration-vibration (V-V), and state-specific dissociation and recombination are used to describe the internal energy model relaxation at high temperatures. In the upper quantum levels, the V-T processes dominate the energy transfer. Dissociation is a reactive process with an activation energy typically over an order of magnitude greater than the energy associated with V-T exchange. Non-reactive kinetic processes tend to bring about an equilibrium distribution in the vibrational manifold, whereas, the dissociation process perturbs it. [5]. Under certain conditions, the V-V processes may play an important role by accelerating the reaction rates. [6].

A diatomic molecule dissociates if its internal energy exceeds the dissociation energy D_0. In general, three limiting dissociation paths are possible [7]; these being: (1) dissociation from the electronic and vibrational ground state due to rotational excitation, (2) dissociation of a non-rotating molecule from the electronic ground state; in other words, the mechanism is breaking of the bond due to molecular vibrations, and (3) dissociation of a non-vibrating and non-rotating molecule during transition from the electronic ground state to the excited repulsive state. None of the above mechanisms exist in pure form, hence the present study considers thermal dissociation according to the mechanism of vibrational excitation with possible rotational excitation or deactivation.

In the work of Josyula and Bailey [8], the generalized depletion equations, considering the state-to-state kinetics of dissociating nitrogen under the restriction of single quantum exchanges, were solved to predict the extent of population depletion in the vibrational manifold. The model helps explain the restricted success of Park's dissociation model in certain temperature ranges of hypersonic flow past blunt body. In the range of 5,000-15,000 K, the depletion model yielded a substantial rate reduction relative to Park's equilibrium rate at lower temperatures and a consistent value at the high end.

The relative importance of V-V exchanges was quantified for dissociation from last quantum level. Multiquantum V-T [9], and V-V processes [10] were modeled by simulating the master kinetic equations coupled to fluid dynamic equations to quantify the thermal and chemical nonequilibrium effects prevalent in hypersonic blunt body. However, the effects of multiquantum exchanges in nitrogen gas for hypersonic nozzle and blunt body flows was not found to be very significant in the thermal relaxation process.

Billing [11, 12] advanced state kinetic modeling by using the semiclassical theory approach to calculate transition rates for atom-diatom and diatom-diatom collisions. This approach was extended by Macheret and Adamovich [13], developing a theory of dissociation of diatomic molecules based on the anharmonicity-corrected and energy-symmetrized forced harmonic oscillator (FHO) quantum scaling [14] in conjunction with free-rotation or impulsive energy-transfer models. The model predicts state specific dissociation rates by accounting for molecular rotation and three-dimensional collisions and has the advantage of being computationally tractable without any adjustable parameters.

In summary, three different approaches to modeling dissociation in nonequilibrium hypersonic flows have been mentioned. The first is the empirical model of Park used in many hypersonic codes today due to its simplicity. The second approach defines the nonequilibium depletion factor based on vibrational state kinetic rates. The third approach incorporates state-specific dissociation rates obtained from the semiclassical dissociation model [13] into a solution of the master kinetic equations coupled to the fluid dynamic equations. The present study considers the third approach: study of state-specific vibrational, dissociation and recombination rates for diatomic nitrogen to describe the thermo-chemical nonequilibrium in hypersonic blunt body flows. The influence of vibrational bias and depletion will be studied. Finally, the result of coupling the state-specific rates to fluid flow equations will be compared to results obtained with simplified dissociation models for a Mach 19 nitrogen flow past a hemisphere cylinder.

ANALYSIS

The global conservation equations in mass-averaged velocity form to simulate a blunt body flow are presented in this section. The inviscid Euler equations were coupled to the master kinetic equations to describe a high temperature hypersonic flow in thermo-chemical nonequilibrium. The nonequilibrium state is simulated for the V-T process, dissociation and recombination processes with state-kinetic rates.

$$\frac{\partial}{\partial t}(\rho_n) + \nabla \cdot (\rho_n \vec{\mathbf{u}}) = \dot{\omega}_n \quad n=0,1,... \tag{1}$$

$$\frac{\partial}{\partial t}(\rho \vec{\mathbf{u}}) + \nabla \cdot (\rho \vec{\mathbf{u}}\vec{\mathbf{u}} - p\bar{\bar{\delta}}) = 0 \tag{2}$$

$$\frac{\partial}{\partial t}(\rho e) + \nabla \cdot [\rho(e + p/\rho)\vec{\mathbf{u}}] = 0 \tag{3}$$

Eqns. 1 to 3 describe the conservation of mass, momentum and energy in the flowfields of interest. Eqn. 1 is discussed further in the following section. Eqn. 2 and 3 represent the conservation of total momentum and energy, respectively. A microscopic kinetic approach was taken by treating the molecule as anharmonic oscillator, calculating the state populations using the master equations.

The conservation Eqn. 1 is written for the mass density in quantum level n. The source term $\dot{\omega}_n$ derived from the vibrational master equations is made up of the relevant energy exchange processes consisting of the V-T, dissociation, and recombination processes. The equations governing the dissociation process considering dissociation to take place from any vibrational level:

$$N_2(n) + M \rightleftharpoons 2N + M \tag{4}$$

For this reaction, the state-specific dissociation and recombination rate coefficients of $N_2 - N_2$ and $N_2 - N$ collisions were implemented in the master kinetic equations described below.

The kinetics of the particle exchanges among the quantum states are simulated using the vibrational master equations, the population distributions are calculated with [15]:

$$\begin{aligned} \dot{\omega}_n = \frac{1}{M}\{\sum_{n'}[k_{VT}(n' \rightarrow n)\rho_{n'}\rho - k_{VT}(n \rightarrow n')\rho_n\rho] + \\ \sum_{n'}[k_{nR}(continuum \rightarrow n)\rho_{N_2}\rho_N^2 - k_{nD}(n \rightarrow continuum)\rho_n\rho_{N_2} + \\ \bar{k}_{nR}(Continuum \rightarrow n)\rho_N^3 - \bar{k}_{nD}(Continuum \rightarrow n)\rho_n\rho_N]\} \end{aligned} \tag{5}$$

The V-T process is associated with the rate coefficient k_{VT} where the molecule loses or gains a vibrational quantum. The de-excitation rate from n' to n for colliding molecules is denoted by $k_{VT}(n' \rightarrow n)$, the inverse collision from $n \rightarrow n'$ by $k_{VT}(n \rightarrow n')$. The dissociation rate coefficient k_{nD} and $\bar{k}_{nD}$ are the state-specific rate coefficients for $N_2 - N_2$ and $N_2 - N$ collisions, respectively. Consistency of the rate coefficient with the principle of detailed balance is enforced. The recombination rate coefficient k_{nR} and $\bar{k}_{nR}$ are the state-specific rate coefficients for $N_2 - N_2$ and $N_2 - N$ collisions, respectively.

Vibrational transition rate coefficients for V-T process are taken from the work of Adamovich and Rich [14] and state-specific dissociation rate coefficients are taken form Macheret and Adamovich [13].

State-Specific Dissociation and Recombination Kinetics

The state specific dissociation rates from the semiclassical theory of dissociation developed by Macheret and Adamovich [13] gives:

$$k_{diss}(v,T) = \left(\frac{8kT}{\pi m}\right)^{0.5} \int_0^\infty \sigma_{diss}(v,U,T) \exp\left(-\frac{U}{T}\right) d\left(\frac{U}{T}\right) \tag{6}$$

where, the expression for the dissociation cross-section assuming free-rotation approximation of diatom-atom collision:

$$\sigma_{diss}(i,E,T) \approx \pi R_m^2 \left(\frac{E}{T}\right)^2 \frac{1}{\pi^2} \int_0^1 dy \int_0^1 d\varepsilon \int_0^\pi d\vartheta \int_0^\pi d\varphi \sum_f P_{if}(E,\varepsilon,\vartheta,\varphi,y) \tag{7}$$

and for the diatom-diatom collision is:

$$\begin{aligned} \sigma_{diss}(i,E,T) \approx \pi R_m^2 \left(\frac{E}{T}\right)^3 \frac{1}{\pi^4} \int_0^1 dy \int_0^1 d\varepsilon_1 \int_0^1 d\varepsilon_2 \int_0^\pi d\vartheta_1 \int_0^\pi d\vartheta_2 \\ \int_0^\pi d\varphi_1 \int_0^\pi d\varphi_2 \sum_f P_{if}(E,\varepsilon_1,\varepsilon_2,\vartheta_1,\vartheta_2,\varphi_1,\varphi_2,y) \end{aligned} \tag{8}$$

In the above, ε, ϑ, and φ are the fractional rotational energy, rotational angle, and angular momentum vector, respectively, E is the total collision energy, U is the potential energy for the 3D molecule-molecule collisions, P_{if} is the probability of the transition process, y is a function of the impact parameter, R_m is the hard sphere diameter, and i is the index of the initial vibrational quantum level, and v is the index of the quantum level. The above equations were derived (See Refs. [11, 12, 13]) by evaluating the probabilities of vibrational transitions including dissociation,

an energy transferred to a classical initially non-vibrating oscillator was calculated. To accomplish this, a potential energy surface was determined and then classical equations of motion were integrated for the system.

A Monte Carlo integration was performed to solve Eqns. 7 and 9, details of which are given in Refs. [11, 12]. The multi-dimensional Monte Carlo integration is implemented by repeated sub routine calls to one dimensional random number generation by using a different seed each time. Thus each subroutine call returns a random value for use as a given parameter of the phase space and also returns a random seed for the random generation of next parameter. Thus a 8 or more dimensional parameter phase space point is created. The process is continued to generate the next phase space point. The reason for this to achieve as much randomness as possible in phase space to avoid any hidden intrinsic correlations in the phase space. We intend to save the phase space data and examine the clustering in it in near future.

The recombination rates are determined by first determining the equilibrium constant at different translational temperatures. At equilibrium, the state populations in the vibrational quantum levels are in a Boltzmann distribution, such that

$$\frac{n[v]}{n[v-1]} = -(\frac{\varepsilon[v]-\varepsilon[v-1]}{kt}) \tag{9}$$

To determine the equilibrium constant, the Saha equation was invoked in the following analysis [16]. The state-specific recombination coefficient is written as

$$k_r[v,T] = k_d[v,T]\frac{2I_{AB}}{\beta h^2}\frac{\lambda_\mu^3}{g_N^2}\exp(\beta(D_0-\varepsilon[v])) \tag{10}$$

where the partition function, $Z_N = \sum_s g_s \exp(\frac{\varepsilon_s}{kT}) \approx g_s$. Here s denotes all the internal states considered for dissociation. The atomic degeneracy, g_s=4.

RESULTS AND CONCLUSIONS

Multiquantum vibrational transitions in Nozzle Flow

Numerical simulation of the highly nonequilibrium flowfields in hypersonic expanding nozzle flows impact predictions of engine thrust in aerospace vehicles. The temperatures in the nozzle throat are at equilibrium and as the flow expands in the nozzle, the vibrational temperature freezes near the throat and the translational temperature drops sharply. $T_{fl} > T$ during the nozzle expansion process results in the cooling of the vibrational energy modes.

Fig. 2 shows the interplay of VT and VV processes in non-equilibrium conditions. Fig. 1, a reference to Fig. 2 is a schematic of a nozzle and the temperature variation along the axial length. Fig. 2 depicts the effects of VT and VV processes for conditions that exist along the length of the nozzle where T_{fl} is high and held constant (vibrational freezing) at 10,000 K and the translational temperature gradually falls along the length of the nozzle, the temperatures at three axial locations selected as, T=5,000 K, 2,500 K, and 1,500 K. As the translational temperature goes down, the contributions due to VT transfers go down but those due to resonant VV exchanges increase: Fig. 2a shows the VT curve above the others (Fig. 2b,c,d) and Fig. 2b shows that in the lower levels, the resonant contributions overtake the VT and non-resonant VV contributions. As the difference in vibrational and translational temperatures increases, see for example Fig. 2d, there is a sharp increase in the resonant VV contributions in the lower levels, then they drop in the intermediate levels, and at the higher levels overtake the non-resonant contributions. It is also noted that VV and VT curves cross over around v=10 for T_{fl}=2,500 K and 5,000 K denoting the end of the plateau region to the beginning of the VT dominant Boltzmann distribution region. However, at all vibrational temperatures, the nonresonant and resonant VV curves cross over around v=10 beyond which the VT effects are dominant.

State-Specific Dissociation and Recombination Rates

Fig. 3 depicts the state specific dissociation rate coefficients of $N_2 - N_2$ collisions given by Ref. [13] at temperatures of 6,100, 10,000, 15,100, and 21,100 K. At all the temperatures considered, the rate coefficient is highest in the upper vibrational levels. To determine the vibrational bias on dissociation, however, it will be necessary to consider the population density in the vibrational levels as well, to be discussed further. There is a scatter in the predictions due to the level spacing and also due to the Monte Carlo method for determining the state specific rate coefficients. Fig. 4 shows the state specific recombination coefficients evaluated in the present study using the method outlined

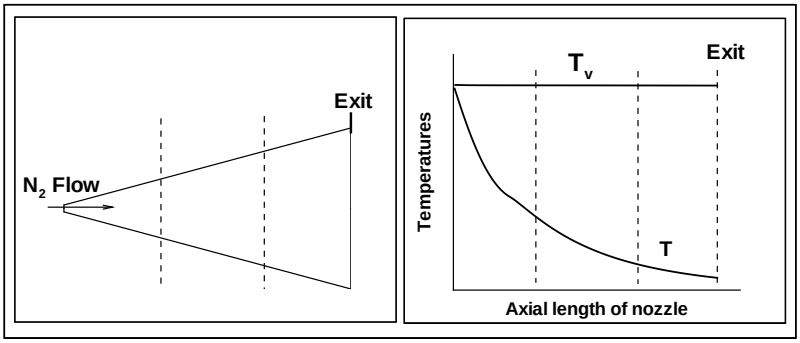

FIGURE 1. Schematic of nozzle and temperature profiles along the axial length

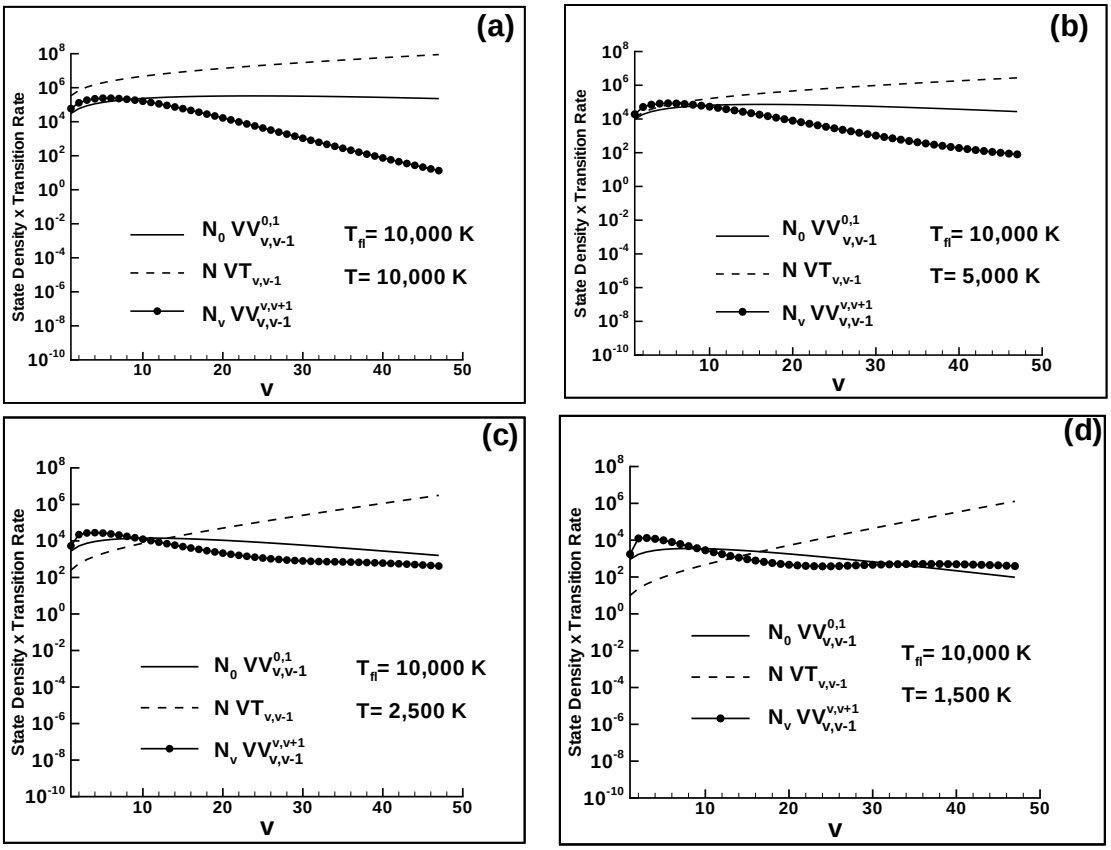

FIGURE 2. Product of number densities and transition rates for non-equilibrium conditions ($T_{fl} > T$) similar to those along different stations along an expanding nozzle, (a) $T_{fl} = 10,000K, T = 10,000K$ (b) $T_{fl} = 10,000K, T = 5,000K$ (c) $T_{fl} = 10,000K, T = 2,500K$, and (d) $T_{fl} = 10,000K, T = 1,500K$

in the earlier section. The highest coefficients at all temperatures are in the upper vibrational levels. Unlike the dissociation process, assessment of bias for the recombination process does not depend on the vibrational population. It is concluded that the recombination is strongly biased to the upper vibrational levels.

With the availability of state-specific dissociation and recombination rate coefficients, it is now possible to assess the effect of vibrational bias on the dissociation. The state-specific dissociation frequency given by the product of the vibrational population and rate coefficient provides an estimate of vibrational bias on dissociation. It is seen from Fig. 5 across the range of temperatures considered in the present study (6,100 to 21,100 K) that the dissociation take place

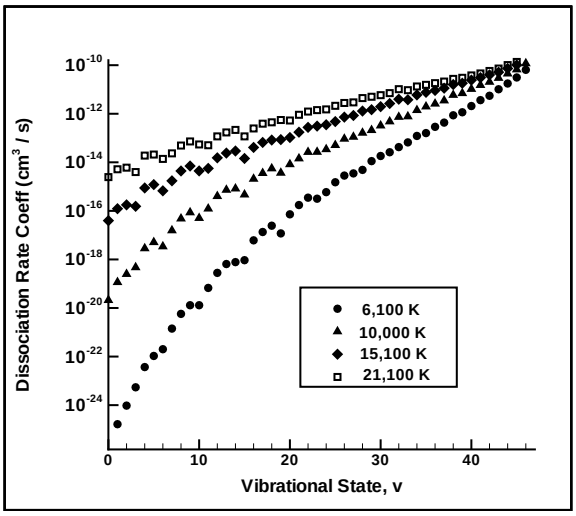

FIGURE 3. State-specific dissociation rate coefficient for $N_2 - N_2$ collisions

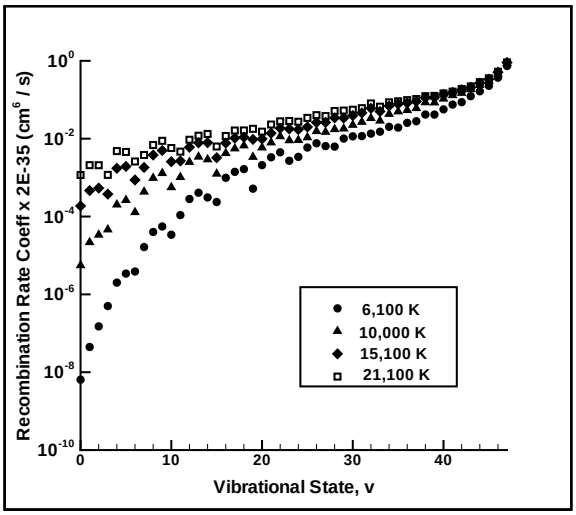

FIGURE 4. State-specific recombination coefficient for $N_2 - N_2$ collisions

primarily from the upper vibrational levels, hence the vibrational bias may be considered to be strong for dissociation.

A Mach 19.83 nitrogen flow past a hemisphere cylinder was considered in this study. The maximum shock temperature was 20,000 K and the dissociation reaction for the nitrogen molecule considered was,

$$N_2 + M \rightleftharpoons 2N + M \tag{11}$$

The radius of the hemisphere was 0.1524 m. Freestream pressure and temperature were 27 Pa and 300 K, respectively.

Three different approaches to modeling dissociation were considered. The first is the empirical model of Park used in many hypersonic codes today due to its simplicity. The chemical source terms were derived from the law of mass action. The reaction rates and equilibrium constants were taken from the work of Park [17]. The vibration-dissociation coupling for the diatomic species was achieved by the two-temperature model suggested by Park [17]: $T_{eff} = \sqrt{TT_v}$ where T_{eff} is the rate-controlling temperature for the forward rate of the dissociation-recombination reactions. The second approach defines the nonequilibrium depletion factor based on vibrational state kinetic rates as discussed in Ref. [2]. The third approach incorporates state-specific dissociation rates obtained from the semiclassical dissociation

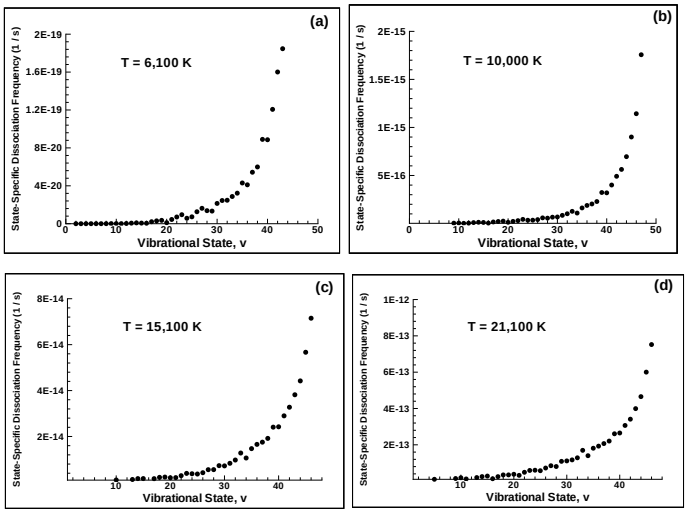

FIGURE 5. Product of vibrational population and dissociation rate coefficient showing effect of bias

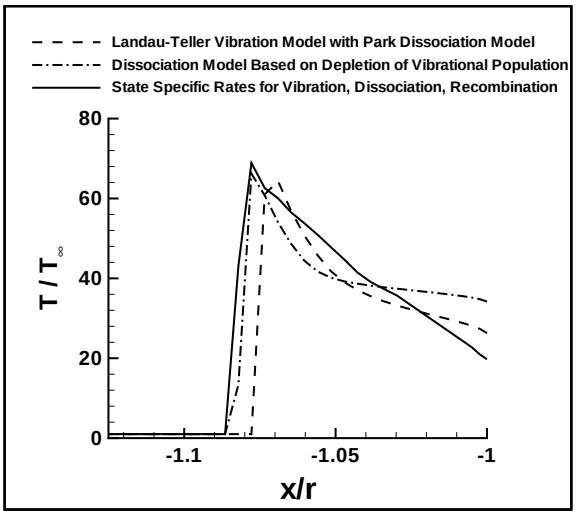

FIGURE 6. Blunt-body flow: Variation of translational temperature in the shock layer for three different dissociation models, M_∞=19.83, p_∞ = 27 Pa, $T_\infty = 300K$, r=0.1524m

model [13] into a solution of the master kinetic equations coupled to the fluid dynamic equations. The master kinetic equations consisted of state-specific vibration, dissociation and recombination rates.

Shown are results from three different methods of modeling, (1) the Landau-Teller vibrational relaxation with Park dissociation model, (2) a dissociation model that accounts for the depletion (3) the present state-specific vibration, dissociation, and recombination implementation of the master kinetic equations coupled to the fluid dynamic equations, as discussed earlier.

An earlier study [2], considered depletion effects in the vibrational quantum levels of a molecule caused by dissociation loss to the continuum. The model reduced the Park's equilibrium dissociation rates in the temperature range of 5,000-15,000 K; in the lower temperature range the reduction was substantial but the rates were consistent with Park's rates in the high temperature regime. Application of the model to a Mach 19.83 pure nitrogen flow predicted an 8% greater shock standoff distance due to lower dissociation rates compared to standard Park's two-temperature model as seen in Fig. 6 which depicts the variation in the translational temperature along the stagnation streamline of the hypersonic blunt body flowfield. The current state-specific dissociation and recombination rate-implementation provides a justification of the earlier depletion model, as seen from the consistency of the shock stand-off distances.

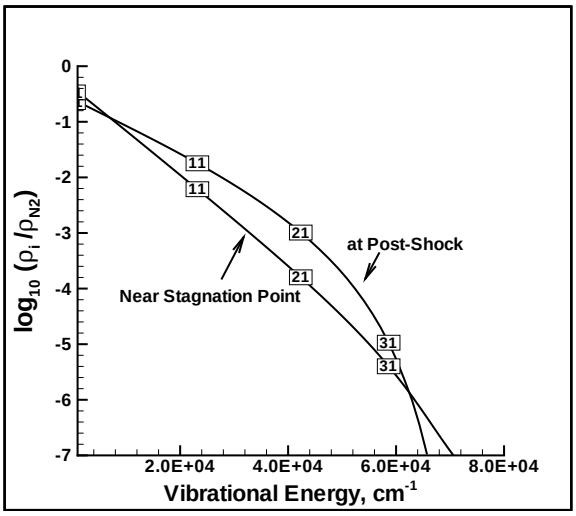

FIGURE 7. Blunt-body flow: Population distribution in the vibrational levels at two locations in the shock layer, M_∞=19.83, p_∞ = 27 Pa, $T_\infty = 300K$, r=0.1524m

Fig. 7 shows the population distribution at two locations along the stagnation streamline - the post shock location and the stagnation streamline. The population distribution near the surface approaches Boltzmann. However, at the high temperature post-shock location, the population distribution is non-Boltzmann with the population decrease at the higher levels depicting significant depletion due to dissociation.

ACKNOWLEDGMENTS

This research was supported under U.S. Air Force Office of Scientific Research contracts monitored by F.Fahroo and J.Schmisseur.

REFERENCES

1. Park, C., *Nonequilibrium Hypersonic Aerothermodynamcis*, John Wiley and Sons, Inc., New York, 1990.
2. Josyula, E., and Bailey, W. F., *Journal of Thermophysics and Heat Transfer*, **15**, 157–167 (2001).
3. Adamovich, I., Macheret, S., Rich, J., and Treanor, C., *AIAA Journal*, **33**, 1064–1069 (1995).
4. Adamovich, I., Macheret, S., Rich, J., and Treanor, C., *AIAA Journal*, **33**, 1070–1075 (1995).
5. Osipov, A. I., and Stupochenko, E., *Combustion, Explosion and Shock Waves, Translated from Fizika Goreniya i Vzryva*, **10**, 303–313 (1974).
6. Osipov, A. I., and Stupochenko, E., *Combustion, Explosion and Shock Waves, Translated from Fizika Goreniya i Vzryva*, **10**, 399–409 (1974).
7. Gordiets, B., Osipov, A., and Shelepin, L., *Kinetic Processes in Gases and Molecular Lasers*, Gordon and Breach Science Publishers, 1988.
8. Josyula, E., and Bailey, W. F., *AIAA Paper 2002-0200* (2002).
9. Josyula, E., Bailey, W., and Xu, K., *AIAA Paper 2004-2468* (2004).
10. Josyula, E., and Bailey, W., *AIAA Paper 2005-5204* (2005).
11. Billing, G., *Computer Physics Communications*, **32**, 45–62 (1984).
12. Billing, G., *Computer Physics Communications*, **44**, 121–136 (1987).
13. Macheret, S., and Adamovich, I., *Journal of Chemical Physics*, **113**, 7351–7361 (2000).
14. Adamovich, I., and Rich, J., *Journal of Chemical Physics*, **109**, 7711–7724 (1998).
15. Josyula, E., *Journal of Thermophysics and Heat Transfer*, **14**, 18–26 (2000).
16. Garrod, C., *Statistical Mechanics and Thermodynamics*, Oxford University Press, New York, 1995.
17. Park, C., *AIAA Paper 85-0247* (1985).